University of Nebraska - Lincoln
DigitalCommons@University of Nebraska - Lincoln

Faculty Publications from the Department of Electrical Engineering

Electrical Engineering, Department of

8-14-2000

All-solid-state electrochromic reflectance device for emittance modulation in the far-infrared spectral region

E. B. Franke
University of Nebraska - Lincoln

C. L. Trimble
University of Nebraska - Lincoln

Mathias Schubert
University of Nebraska - Lincoln, mschubert4@unl.edu

J. A. Woollam
University of Nebraska - Lincoln

Follow this and additional works at: http://digitalcommons.unl.edu/electricalengineeringfacpub

Part of the Electrical and Computer Engineering Commons

Franke, E. B.; Trimble, C. L.; Schubert, Mathias; and Woollam, J. A., "All-solid-state electrochromic reflectance device for emittance modulation in the far-infrared spectral region" (2000). *Faculty Publications from the Department of Electrical Engineering.* Paper 12.
http://digitalcommons.unl.edu/electricalengineeringfacpub/12

This Article is brought to you for free and open access by the Electrical Engineering, Department of at DigitalCommons@University of Nebraska - Lincoln. It has been accepted for inclusion in Faculty Publications from the Department of Electrical Engineering by an authorized administrator of DigitalCommons@University of Nebraska - Lincoln.

All-solid-state electrochromic reflectance device for emittance modulation in the far-infrared spectral region

E. B. Franke[a)]
Center for Microelectronic and Optical Materials Research, and Department of Electrical Engineering, University of Nebraska-Lincoln, Nebraska 68588-0511 and Institut für Oberflächenmodifizierung Leipzig e.V., Permoserstr. 15, 04318 Leipzig, Germany

C. L. Trimble, M. Schubert, and J. A. Woollam
Center for Microelectronic and Optical Materials Research, and Department of Electrical Engineering, University of Nebraska-Lincoln, Nebraska 68588-0511

J. S. Hale
J. A. Woollam Co. Inc., Suite 102, 645 M Street, Lincoln, Nebraska 68588

(Received 7 February 2000; accepted for publication 19 June 2000)

All-solid-state electrochromic reflectance devices for thermal emittance modulation were designed for operation in the spectral region from mid- to far-infrared wavelengths (2–40 μm). All device constituent layers were grown by magnetron sputtering. The electrochromic (polycrystalline WO_3), ion conductor (Ta_2O_5), and Li^+ ion-storage layer (amorphous WO_3), optimized for their infrared (IR) optical thicknesses, are sandwiched between a highly IR reflecting Al mirror, and a 90% IR transmissive Al grid top electrode, thereby meeting the requirements for a reversible Li^+ ion insertion electrochromic device to operate within the 300 K blackbody emission range. Multicycle optical switching and emittance modulation is demonstrated. The measured change in emissivity of the device is to 20%. © *2000 American Institute of Physics.* [S0003-6951(00)01733-2]

In the past, electrochromic devices (ECDs) were primarily investigated for applications such as transmittance modulating daylight and solar control window coatings for buildings (smart windows), optical displays, and reflectance modulating automobile rear-view mirrors (see for instance Ref. 1). ECDs are multilayer structures, and constituents are assembled as follows: substrate/transparent electrode/ion-storage layer/ion conductor/electrochromic layer/transparent electrode. Small ions (typically H^+ or alkali ions) are inserted into the device structure via electrochemical processes. Ions are able to move from the electrochromic into the ion-storage layer and back, driven by a voltage applied between the electrodes.

Electrochromic devices can be also used for surface emissivity control by switching between a high or low irradiative surface state for infrared, (IR) wavelengths. Surface emissivity characteristics are related to the blackbody emission, and depend therefore on temperature. Near room temperature the maximum of the blackbody emission spectrum is at 10 μm, and an emittance modulation device (EMD) must be operational in the mid- to far-infrared spectral region (IR: 2–40 μm). IR–EMDs are of interest for thermal control in satellites positioned in low earth orbit, where the satellite temperature is close to 300 K. Thermal control is accomplished by balancing energy dissipated by heat against the energy emitted as IR radiation.[2] Existing visible and near-IR range EMDs are useless to perform immediately at far-IR wavelengths, because of (i) highly absorbing electrode materials, and (ii) the optical response of the device constituents at long wavelengths, which differs from the visible and near-infrared range due to free carrier and lattice contributions. Standard visible and near-IR range ECDs employ electrode materials which are highly reflective for long wavelengths due to free-carrier effects in highly conductive films.[3] Wide-spaced metal grids are alternative IR electrodes and should have a transmittance of at least 90%. Different types of IR–EMDs have been suggested. One[1] is based on a diffusion controlled ECD where the electrochromic layer is located on top of an ion-permeable (and possible transparent) electrode (typically a metal grid). The ion conductor, ion-storage layer, and a highly reflecting electrical conductor are underneath the metal grid. The ions are proposed to diffuse through the metal grid electrode in order to achieve color change in the electrochromic layer. This concept is based on a device structure originally proposed by Baucke[4] for visible range ECDs which do not transmit radiation, but change reflectivity as needed for car rear-view mirrors.

A different type of IR–EMDs employs highly IR-absorbing polymers as ion-conducting materials. Such devices were built by Topart and Hourquebie.[5] Device performance was optimized for a spectral region from 0.2 to 20 μm with a high dynamic range, and coloring and bleaching reproducibility after voltage switching.

Trimble *et al.*[6] also reported on IR–EMD structures with a thick polymer as an ion conductor layer. However, a low-doped silicon wafer was used as an IR transmissive top electrode, which deteriorates the optical device performance due to high absorption in the silicon wafer.

Cogan *et al.*[7] theoretically proposed an EMD for the wavelength region from 2 to 5 μm with two conducting grids as bottom and top electrodes, a highly emissive substrate, and an ion-conducting polymer. Cogan *et al.*[7] also tested crystalline (*c*) WO_3 and amorphous (*a*) WO_3 in half devices

[a)]Electronic mail: franke@engrs.unl.edu

 © 2000 American Institute of Physics

TABLE I. Growth sequence and parameters (sputter power, P_{sp}, pressure; p, temperature; T, argon flux; f_{Ar}, oxygen flux; f_{O_2}, nominal thickness; d used for electrochromic device constituent depositions.

Thin film	P_{sp}	p (mTorr)	T (°C)	f_{Ar} (sccm)	f_{O_2} (sccm)	d (nm)
Al	40 W (dc)	5	25	20	···	40
a-WO_3	35 W (dc)	15	25	35	4.5	160
Ta_2O_5	100 W (rf)	13	375	20	7	350
c-WO_3	35 W (dc)	15	375	35	4.5	160
Al	40 W (dc)	5	25	20	···	40

as IR electrochromic and ion-storage layer, respectively. But so far, no experimental performance of complete devices has been reported.

In this letter the cell structure and performance of the experimentally built all-solid-state electrochromic devices for emittance modulation in the spectral region from 2 to 40 μm with the layer sequence glass substrate/Al electrode/amorphous WO_3/Ta_2O_5/polycrystalline WO_3/Al grid electrode are reported. The device design is based on the Baucke concept.[4] However, the design was modified with respect to layer stack geometry, avoiding a diffusion mechanism for coloring and bleaching of the electrochromic layer. The electrochromic, ion conductor, and storage layers with thicknesses optimized for IR operation are sandwiched between a highly IR-reflecting Al bottom, and a 90% IR-transmissive Al grid top electrode. Ion-storage layer and bottom electrode contribute to the optical device performance, because IR radiation can penetrate through all device constituents, except for the bottom electrode. The bottom electrode needs to be in thermal contact to the surface, whose emissivity is desired to be controlled.

It was proposed that c-WO_3 could be used for IR–EMDs, where the emittance modulation occurs by increasing (decreasing) the free electron concentration during element reduction (oxidation) upon ion insertion (extraction).[8–10] In our devices ion-storage and ion-conductor layers should be transparent to IR wavelengths. a-WO_3 is an IR candidate for a Li^+ ion-storage layer, because a-WO_3 remains nearly transparent over a wide IR spectral region, independent of the inserted Li^+ concentration.[11] The IR optical properties of tantalum oxide have been studied previously,[12] because the n and k spectra are prerequisites for IR–EMD design when tantalum oxide is used as an ion conductor.

Using optical constants measured on individual constituent layers, the optical modulation performance of our IR–EMDs was simulated, and then optimized by changing the constituent layer thicknesses, as reported in a prior publication.[13] The devices were made in a two-step vacuum deposition process. The Li^+ were electrochemically inserted into the finished device structure through the top metal grid. The reflectance modulation was measured in the spectral region from 2 to 40 μm using a commercial Fourier-transform IR spectrometer, with an angle of incidence of 11°.

All device constituents were deposited by direct current (dc) or radio frequency (rf) magnetron sputtering in a high-vacuum deposition chamber with a typical background pressure of 3×10^{-6} Torr. Glass slides were used as substrate material. Table I gives the deposition conditions of the various films used to manufacture the devices. *In situ* ellipsometry was used to monitor the layer growth, and to measure the device constituent layer thicknesses.

Electrochemical Li^+ intercalation was performed in a 1.0 molar solution of $LiClO_4$ in propylene carbonate using a potentiostat. The electrochemical cell contains a platinum foil as a counter electrode and a saturated calomel reference electrode. The potentiostat controls the voltage at the working electrode (sample) by varying the counter electrode potential.

A photolithographic process was used to manufacture the IR-transmissive top electrode aluminum metal grid. The mask for the grid was made for 10 μm linewidths and a 500 μm line repeat period. The IR transmission was estimated to be 90%.

Before assembly of the device, the constituents were deposited as single films onto [001] silicon substrates. Glancing-angle-of-incidence x-ray diffraction was used to study phase content and crystallinity of the thin films.[12,14] As-deposited crystalline WO_3 films possess a monoclinic crystal structure. However, after Li^+ insertion an irreversible phase transformation occurred resulting in a cubic $Li_xW_{(1-x)}O_3$ (tungsten bronze) structure, which changed to a tetragonal $Li_xW_{(1-x)}O_3$ phase after Li^+ extraction. The irreversibility of the phase transformation is caused by a certain amount of Li^+, which remains in the WO_3 after ion extraction.[1,15]

The tantalum oxide thin films were found to be amorphous in our deposition regime. However, the deposition process was optimized considering microporosity within the thin films. Microporosity could be caused by pinholes reaching through the film from one interface to the next. The pinholes could cause electron conductivity and therefore a failure of operation of the ion conductor. Tantalum oxide thin films deposited at temperatures higher than 200 °C, and oxygen flux rates above 7 sccm showed considerably smaller microporosity than those grown at lower temperatures and smaller oxygen flux rates.[12]

The optical properties of all device constituents were investigated by spectroscopic ellipsometry in the spectral region from 0.03 to 8.5 eV (0.15 to 40 μm).[12,14,16] In addition to evaluating material dielectric functions, thin-film microporosity was studied and quantified during analysis of the ellipsometric spectra. Optical response was also measured on half devices, consisting of either substrate/electrode/electrochromic layer, or substrate/electrode/ion-storage layer.[6] With this assembly we determined the change in dielectric function of the electrochromic and ion-storage layers after Li^+ insertion. The results from these optical investigations were used for device model calculations.[13]

The layer structure of the IR–EMDs used in this work is shown in Fig. 1. The vacuum process was interrupted after deposition of the bottom electrode to mask one edge of the electrode material for electrical contacts.

Figure 2 shows the reflectance modulation of our IR–EMD after switching the voltage from -2 (colored) to $+2$ V (bleached). The maximum reflectance modulation occurred in the spectral region between 5 and 20 μm and was estimated to be 25%. However, there is a strong absorption feature near $\lambda=10\,\mu$m caused by characteristic lattice absorption contributions from each metal oxide (c-WO_3, a-WO_3,

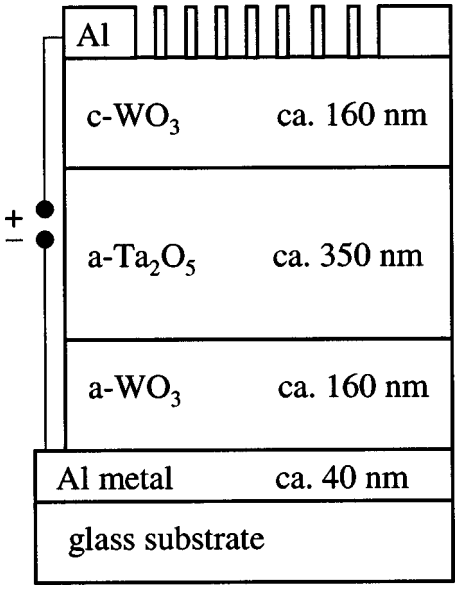

FIG. 1. Structure of the electrochromic device manufactured for thermal emittance modulation (not to scale).

a-Ta_2O_5).[12,14] The strong lattice absorption limits the present device performance. Smaller film thicknesses or higher film quality (smaller lattice resonance linewidth) could improve device performance in this spectral region. Structures in the spectral region from 15 to 40 μm are due to thickness dependent interference effects, which are mainly caused by the thick a-Ta_2O_5 ion-conductor layer. Devices with thinner Ta_2O_5 layer thickness usually failed because of electrical shorts between the ion-storage and electrochromic layers. The IR–EMDs were cycled between the colored and the bleached state by switching the voltage several times. No significant changes in the reflectance spectra at the two extreme were observed. One cycle was complete after approximately 30 min.

The IR–EMDs show their highest reflectance with Li^+ in the c-WO_3 layer. This is opposite to the reflectance modulation behavior predicted in Ref. 16, which claims the highest reflection state with Li^+ in the a-WO_3 layer. However, the calculations in Ref. 16 were made using constituent layer optical properties assuming ideal switching behavior. From secondary neutral mass spectroscopy measurements of the Li^+ depth profile of our device it was found, that a certain amount of Li^+ always remain in the top c-WO_3 layer, even after ion extraction. The optical switching in our device is mainly caused by the lower or higher reflectance of the c-WO_3 layer depending on its Li^+ concentration and is almost independent from the optical properties of the remaining layer stack below the c-WO_3 layer. IR–EMD reflectance calculations, performed by accounting for noncomplete reversible ion insertion/extraction process, confirmed the reflectance modulation behavior shown in Fig. 2.

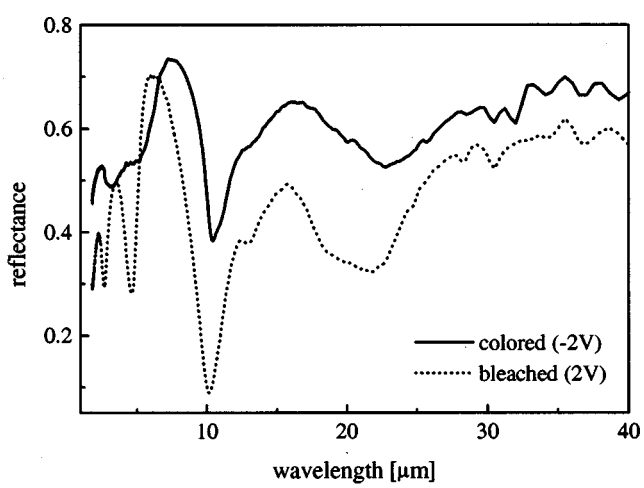

FIG. 2. Reflectance modulation of the electrochromic device after switching the voltage from −2 (colored) to +2 V (bleached). Device reflectance is measured at 11° angle-of-incidence and against gold reflection standard. The device shows its highest reflectance with Li^+ in the c-WO_3 layer.

The emittance E of the device in its different states (bleached, colored) relative to the blackbody spectra at temperature T is given by

$$E=\frac{\int_{\lambda_1}^{\lambda_2}[1-R(\lambda)]M_b(\lambda,T)d\lambda}{\int_{\lambda_1}^{\lambda_2}M_b(\lambda,T)d\lambda}, \tag{1}$$

where $R(\lambda)$ is the device reflectance, and $M_b(\lambda,T)$ is the blackbody spectral emittance at $T=300\,\mathrm{K}$, and for $\lambda_1=2\ \mu$m and $\lambda_2=40\ \mu$m. The IR–EMD shown in Fig. 2 presents an emittance modulation from 0.4 to 0.59. The dynamic range between the high and low emissivity state is ~20%, and the ratio is 1.5.

The authors acknowledge K. Zimmer and E. Salamatin for providing the grid masks. The authors thank Tariqul Islam for help during photolithography. This work was supported by BMDO DSAG60-98-C-0054, NASA Glenn Research Center NAG3-2219, and NASA Epscor NCC5-169.

[1] C. G. Granqvist, *Handbook of Inorganic Electrochromic Materials* (Elsevier, Amsterdam, 1995).
[2] D. G. Gilmore, *Satellite Thermal Control Handbook* (The Aerospace Corporation Press, El Segundo, CA, 1994), p. 4.
[3] A. Gerouki and R. B. Goldner, Mater. Res. Soc. Symp. Proc. **548**, 679 (1999).
[4] K. Baucke, Sol. Energy Mater. **16**, 67 (1987).
[5] P. Topart and P. Hourquebie, Thin Solid Films **352**, 243 (1999).
[6] C. L. Trimble, M. J. DeVries, J. S. Hale, D. W. Thompson, T. E. Tiwald, and J. A. Woollam, Thin Solid Films **347**, 1 (1999).
[7] S. F. Cogan, R. D. Rauh, J. D. Klein, and T. D. Plante, *Electrochemical Society Proceedings* (Electrochemical Society, Pennington NJ, 1995), Vol. 94-2, p. 269.
[8] R. B. Goldner and R. D. Rauh, Proc. SPIE **428**, 38 (1983).
[9] R. B. Goldner, F. Arntz, G. Berera, T. E. Haas, G. Wei, K. K. Wong, and P. Yu, Proc. SPIE **1536**, 34 (1991).
[10] S. F. Cogan, T. D. Plante, M. A. Parker, and R. D. Rauh, J. Appl. Phys. **60**, 2735 (1986).
[11] S. F. Cogan, R. D. Rauh, J. D. Klein, and T. D. Plante, Proc. SPIE **1149**, 2 (1989).
[12] E. Franke, M. Schubert, C. L. Trimble, M. J. DeVries, J. S. Hale, J. A. Woollam, and F. Frost (unpublished).
[13] J. S. Hale and J. A. Woollam, Thin Solid Films **339**, 174 (1999).
[14] M. J. DeVries, C. L. Trimble, T. E. Tiwald, D. W. Thompson, J. A. Woollam, and J. S. Hale, J. Vac. Sci. Technol. A **17**, 2906 (1999).
[15] Q. Zhong, J. R. Dahn, and K. Colbow, Phys. Rev. B **46**, 2554 (1992).
[16] J. S. Hale, M. J. DeVries, B. Dworak, and J. A. Woollam, Thin Solid Films **313–314**, 205 (1998).